Journal of Engineering Physics and Thermophysics, Vol. 75, No. 5, 2002

TRANSFORMATION OF THE MAGNETOSTATIC-FIELD SPATIAL HARMONIC IN A MAGNETIC FLUID LAYER

A. N. Vislovich and A. B. Sukhotskii

UDC 537.84

A plane-parallel layer of magnetic fluid is placed in an inhomogeneous magnetostatic field formed by a plane system of permanent magnets periodically distributed in space. The change in the field characteristics in the region of reflection (between the system and the layer) and screening (behind the layer) has been investigated. An approximate theoretical description of the observed effect is given.

Introduction. The theory of magnetostatic fields in magnets is a classical branch of the electrodynamics of continua. Among the large number of field distributions for concrete geometries, one can single out several fundamental fields widely used in physical theories, measuring methods, and technical evaluations, for example, the field of a homogeneously magnetized (polarized) ellipsoid [1]. The field of the plane-parallel magnetizable layer in an inhomogeneous external field of the type of "spatial harmonic" considered in the present paper can be classified among such kinds of distributions. The behavior of an individual component of the field forms the basis for modeling a fairly wide range of phenomena and technical devices (magnetic screens, suspensions, nondestructive testing devices, etc.).

Magnetic fluid is a convenient model for theoretical and experimental studies, since this medium fits into the category of anhysteretic strongly magnetizable substances, and the fluid-layer thickness is an easily variable parameter. The study of the inhomogeneous magnetostatic field scattering is of interest for determining the stability characteristics of ferrofluid dispersions, since the "spatial harmonic"-type distribution features exponential inhomogeneity of the field modulus and can cause a disturbance in the homogeneous dispersion distribution in the fluid sample. Consequently, this field is not only a probing, but also a test factor "deforming" the structure of the magnetic fluid.

1. Description of the Experimental Facility. As a magnetic field source, we used a plane periodic magnetic system 1 composed of elementary magnets made from a hard magnetic material in the form of rectangular parallelepipeds extended along the *y*-axis and magnetized perpendicular to this axis (Fig. 1). The spatial period of the system is composed of four elementary cells (fourth-order system) with λ = 80 mm, l_a = 20 mm, and an elementary cell width of 20 mm. The overall dimensions of the system are 160 × 160 mm.

A cell 2 filled with a magnetic fluid is placed on the magnet. In our experiments, we use cells of a different height with two limiting horizontal plates 3 and 4 made of organic glass. The geometric parameters of the cells are as follows: length (along the *x*-axis) of 60 mm, width (along the *y*-axis) of 50 mm, heights l_c = 3.3 mm, 13, 16.7, and 19.7 mm, thicknesses of the limiting horizontal plates of the cell of 3.1 mm. The upper limiting plate 4 excludes perturbations on the magnetic fluid surface when a cell completely filled with a magnetic fluid is placed on the magnetic system,

As a magnetic fluid, we used a colloidal suspension of magnetite particles in transformer oil. The dependence of its magnetization on the magnetic field strength is given in Fig. 2a. To describe the magnetization curve, it is convenient to use the equation [5]

$$M = M_s H/(H_h + H) . \tag{1}$$

According to (1), the H/M ratio and H are related by a linear dependence (Fig. 2b). Approximating the experimental data by a straight line, we find the parameters of Eq. (1): M_s = 54.44 kA/m and H_h = 17.49 kA/m.

2. Magnetostatic Field Distribution in a Linearly Magnetizable Layered Medium. We assume that for an approximate description of the field distribution the space is divided into three plane-parallel unbounded layers (a', a), (a, c), and (c, c') and two semispaces ($-\infty$, a') and (c', $+\infty$) (Fig. 1).

Belarusian State University of Technology, Minsk; email: wislowich@mail.ru. Translated from Inzhenerno-Fizicheskii Zhurnal, Vol. 75, No. 5, pp. 88–95, September–October, 2002. Original article submitted March 13, 2002.

1062-0125/02/7505-1116$27.00 ©2002 Plenum Publishing Corporation

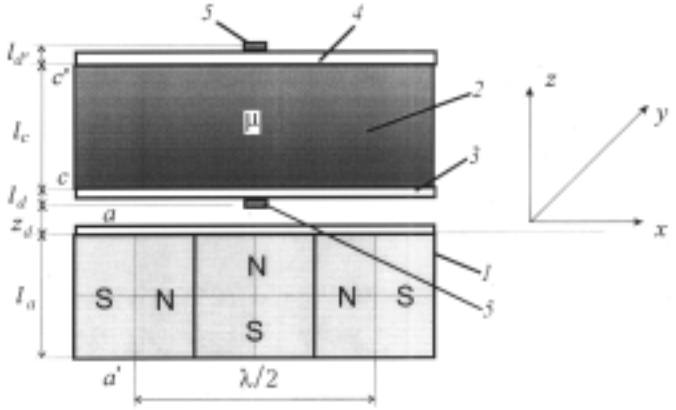

Fig. 1. Schematical representation of the facility: 1) magnetic system; 2) cell; 3, 4) limiting plates; 5) sensor of the magnetic induction meter.

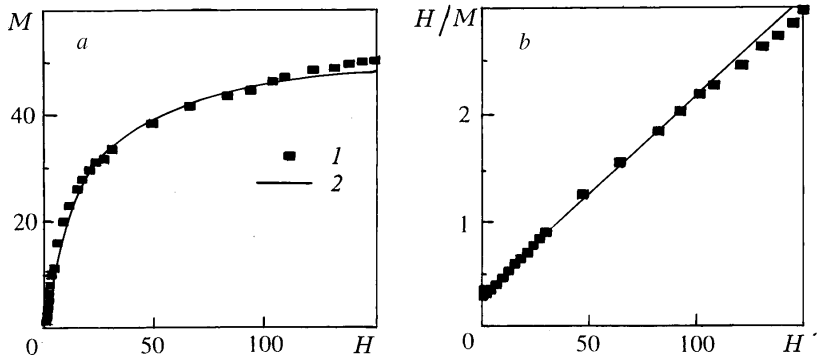

Fig. 2. Dependence of the magnetic characteristic of the fluid [a) magnetization; b) inverse magnetic susceptibility] on the magnetic field strength: [1) experiment; 2) linear-fractional dependence].

The distribution of components of the constant component of magnetization in the field source (a', a) can be given in the form of a Fourier expansion

$$M_x = -\sum_n M_{xn} \sin(nx), \quad M_z = \sum_n M_{zn} \cos(nx), \quad n = 1, 2, 3, \ldots . \tag{2}$$

We use dedimensionalized spatial variables and, as a distance scale, we choose the quantity $\lambda/2\pi$. Within each cell $M_x = M_f$ = const and $M_z = M_f$ = const and the magnetization orientation alternates in accordance with Fig. 1.

The field generated by the first harmonic (n = 1) of distribution (2) in a linearly magnetizable layered medium can be given in the form [6]

$$\mathbf{H}^{(i)} = L_i \exp(z_i - z)(\mathbf{i}_x \sin x + \mathbf{i}_z \cos x) + R_i \exp(z - z_i)(-\mathbf{i}_x \sin x + \mathbf{i}_z \cos x), \tag{3}$$

where the constants L_i and R_i (base projections of the field for the ith layer) are determined from the conditions at the interfaces between layers with different magnetic permeabilities of the substance μ_i that are constant within each layer. In the absence of magnetized layers in the upper semispace (a, $+\infty$) the field is only determined by the L-projection

$$\mathbf{H}^{(0)} = L_a \exp(-z)(\mathbf{i}_x \sin x + \mathbf{i}_z \cos x), \quad |\mathbf{H}^{(0)}| = H^{(0)} = \xi H_h, \tag{4}$$

where $\xi = \xi_a \exp(-z)$; $\xi_a = L_a/H_h$.

From (1) it follows that at values of the dimensionless variable $\xi << 1$ ("weak field") the layer is in the region of linear magnetization and at $\xi >> 1$ ("strong field") it is in the saturation region.

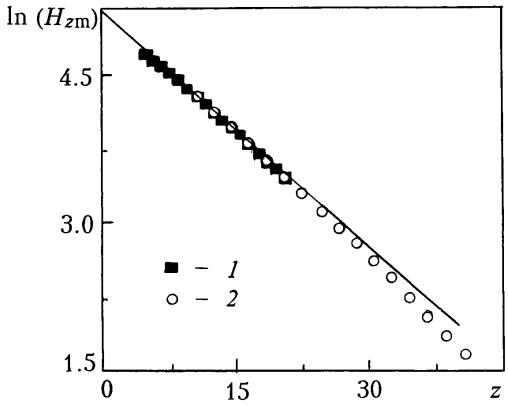

Fig. 3. Logarithmic dependence of the field strength on the *z*-coordinate: [1) at a distance of 5 mm from the edge; 2) in the center of the system].

To determine the parameter L_a, we measured the dependences of the field strength, presented on a logarithmic scale in Fig. 3, on the distance to the surface of the system at various positions of the reference point of the *z*-coordinate. It is seen that at distances of $z \geq 5$ mm the role of the higher harmonics becomes negligibly small and the plot has a rectilinear asymptotics. Because of the finiteness of the dimensions of the magnetic system, at $z \geq 17$ mm near the edge and at $z \geq 21$ mm in the center of the system the plot begins to somewhat deviate from the straight line. Consequently, in the region of $5 \leq z \leq 21$ mm the field of the source used is described, with a good degree of accuracy, by the spatial harmonic (4) for which L_a = 168.5 kA/m and ξ_a = 9.63.

In the presence of a layered linearly magnetizable medium the base projections of the field at either side of the interface between media with a different magnetic permeability is determined as

$$q_i = \frac{L_i}{L_i^-} = \frac{1 - r_i}{1 + r_i s_{i-1} \exp(-2l_i)}, \quad s_i = \frac{R_i^-}{L_i^-} = \frac{r_i + s_{i-1} \exp(-2l_i)}{1 + r_i s_{i-1} \exp(-2l_i)}, \tag{5}$$

where $r_i = (\mu_i - \mu_{i+1})/(\mu_i + \mu_{i+1})$; $L_i^- = L\ (z = z_i - 0)$; $L_i = L\ (z = z_i + 0)$.

Relations (5) are recurrent formulas by which the coefficients q_i and s_i for any semispace are determined in terms of layer thicknesses l_i and magnetic permeabilities μ_i in a given semispace. For example, parameters for the semispace of $z \geq z_j$ can be expressed in terms of values with indices $i \leq j$. For the edge boundary, the condition $l_1 \to \infty$ takes place and, as follows from (5), $s_1 = r_1$ and $q_1 = 1 - r_1$. The boundary number *i* increases with decreasing boundary coordinate z_i.

Consider the spatial harmonic transformation under interaction with a magnetic layer (c, c') of thickness l_c with magnetic permeability μ. For the coefficient of field reflection from the layer at $r_{c'} = s_{c'} = -r_c \equiv -r$ we obtain

$$s = \frac{R_c^-}{L_c^-} = \frac{r\,[1 - \exp(-2l_c)]}{1 - r^2 \exp(-2l_c)}. \tag{6}$$

The coefficient of field transmission through the layer is equal to the product of the coefficients of transmission through the boundaries of the semispaces connected to the layer boundaries. Taking into account that

$$q_c = \frac{1 - r}{1 - r^2 \exp(-2l_c)}, \quad q_{c'} = 1 + r, \tag{7}$$

we have

$$q = \frac{L_{c'}}{L_c^- \exp(-l_c)} = q_c q_{c'} = \frac{1 - r^2}{1 - r^2 \exp(-2l_c)}. \tag{8}$$

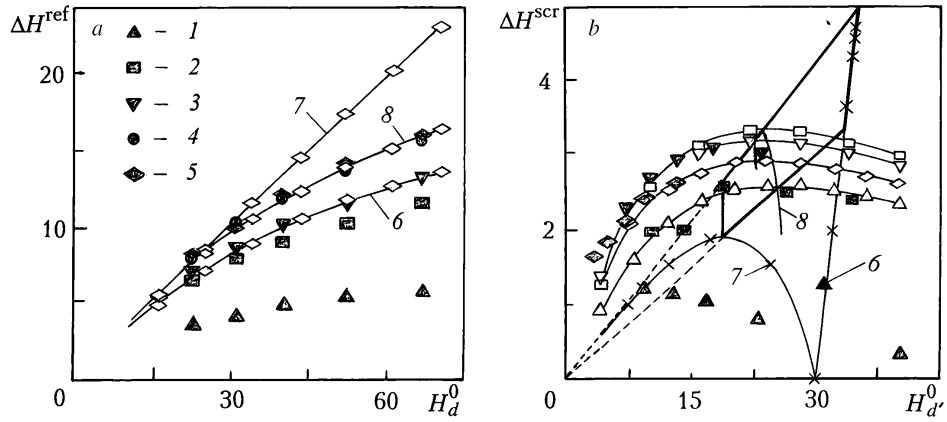

Fig. 4. Dependence of changes in the field in the regions of reflection (a) and screening (b) on the characteristics of the layer position for various layer thicknesses: [1) 3.3; 2) 8.3; 3) 13.4; 4) 16.7; 5) 19.7 mm; (a) 6 and 7) calculation by the one-layer model for $\mu_* = \mu_c$ and $\mu_* = \mu_{c'}$, respectively; (b) 6 and 7) conditional maximum curve calculated by the one-layer model; 8) calculation by the multilayer model]. Dark symbols — results of measurements, light symbols of the same shape — results of calculations.

From (8) the expression for the coefficient of field screening by the layer

$$\Delta q \equiv 1 - q = \frac{r^2 [1 - \exp(-2l_c)]}{1 - r^2 \exp(-2l_c)} \tag{9}$$

follows.

3. Experimental Investigation of the Magnetostatic-Field Spatial Harmonic Transformation by a Magnetizable Layer. A nonmagnetic plane-parallel plate specifying the distance z_d of the sensing element of the magnetic induction meter from the source surface is placed on the magnetic system. The probe moves over the plate surface along the x-coordinate, and the z-component of the magnetic field strength, whose maximum value (amplitude) for the monoharmonic field is equal to the field modulus $H_d^{(0)}$, is determined. With the same position of the probe over it on the spacers a cell with a magnetic fluid is placed and the field modulus in the presence of the cell is determined. The change in the meter reading in this case (reflection effect) $\Delta H_d^{\text{ref}} = H_d - H_d^{(0)}$ is due to the field reflection from the magnetizable layer. The position of the interface c is determined by the parameter $z_c = z_d + l_d$ (Fig. 1). Changing z_c (moving the cell along the z-axis), one can change the external field strength at the layer input. In so doing, the sensing element of the detector in the course of measurements was located at a constant distance l_d = 3.4 mm from the magnetizable layer boundary. Figure 4a shows the dependences of the reflection effect on the external field strength $H_d^{(0)}$ for various thicknesses l_c of the magnetizable layer.

Analogous measurements have been made for the case where the magnetizable layer was situated between the field source surface and the induction meter probe. In this case, the decrease in the field $\Delta H_{d'}^{\text{scr}} = H_{d'}^{(0)} - H_{d'}$ is due to the screening effect of the layer. The measurement data for the screening effect versus the external field strength at the layer output are given in Fig. 4b. The sensing element of the detector is located at a constant distance $l_{d'} = l_d$ = 3.4 mm from the magnetizable layer boundary c'; therefore, the position of the upper boundary of the layer c' is determined by the parameter $z_{c'} = z_d - l_{d'}$.

For the magnetic system made from a hard magnetic ferromagnet, the permeability can be assumed to be approximately equal to unity. In this case, the secondary reflection of the field from the source (a-layer) can be neglected, and it can be assumed that the L-field in the layer (a, c) remains unchanged when the c-layer is introduced. This approximation is fulfilled under the experimental conditions, which permits considering the field in the layer (a, c) to be equal to the external field $L = H^{(0)} = \xi H_{\text{h}}$. Taking into account that in the semispace $(c', +\infty)$ the R-field is absent, to determine the base projections by the measurement data, we have

$$L_c^- = H_d^{(0)} \exp(-l_d), \quad R_c^- = \Delta H_d^{\mathrm{ref}} \exp(l_d), \quad L_{c'} = H_{d'} \exp(l_{d'}). \tag{10}$$

These expressions are the basis of the calculation formulas for experimentally determined values of the transformation coefficients

$$s = \Delta H_d^{\mathrm{ref}} / H_d^{(0)} \exp(2l_d), \quad \Delta q = \Delta H_{d'}^{\mathrm{scr}} / H_{d'}^{(0)}. \tag{11}$$

4. Quasi-Linear Models for Calculating the Transformation Coefficients in the Nonlinearly Magnetizable Medium. The linear theory offers, for calculating the reflection and screening coefficients, expressions where the substance permeabilities μ are constant within the layer. However, under the experimental conditions μ_c in the vicinity of the boundary c markedly differs from $\mu_{c'}$ in the vicinity of the boundary c'. For example, the external field strength within the layer at l_c = 19.7 mm changes from 108 kA/m at the lower boundary to 27 kA/m at the upper boundary of the layer (Fig. 3). The corresponding permeability values are from μ_c = 1.4 to $\mu_{c'}$ = 2.4.

The simplest method for describing the phenomenon of field transformation in a nonlinearly magnetizable medium consists of the assumption that within the layer the permeability is constant and equal to a certain effective value of μ_* lying in the range of changes in the actual permeability. This approach is hereinafter referred to as the *single-layer transformation model*. As the strength at the layer input is changed, there is also a change in μ_* in the general case, and in the single-layer model the problem of choosing the effective value of permeability exists. Consider the simplest variants: (a) the maximum value of $\mu_{c'}$ attainable in the vicinity of the boundary c' is chosen and (b) the minimum value of μ_c is chosen. By the maximum and minimum values of μ_* from (6) and (9) one can determine intervals in which transformation coefficients are contained, since they are monotonic functions of permeability.

As the layer thickness is decreased, the range of change in the permeability inside the layer narrows and, consequently, the uncertainty of the description on the basis of the one-layer model decreases. Therefore, a more detailed approach for taking into account the nonlinearity of the law of magnetization in wide layers is to conditionally split the layer into N sublayers of thickness l_c/N each. Within each sublayer, μ_* can be assumed to be constant and equal to the mean value of $\mu_{i*} = (\mu_i + \mu_{i-1}^-)/2$, where i = 1, ..., N + 1; μ_1 = 1 is the permeability of the semispace (c', ∞); μ_{N+1}^- = 1 is the permeability of the layer (a, c).

Upon transmission through the sublayer boundaries μ_* changes stepwise. In this case, $s = s_{N+1} \equiv s_c$ is calculated as the coefficient of reflection from the multilayer sample by the second of formulas (5). The transmission coefficient through the layer is determined from (5) as

$$q = q_1 q_2 \ldots q_i \ldots q_{N+1}, \tag{12}$$

where $q_1 = q_{c'}$; $q_{N+1} = q_c$.

Using (1) for the magnetization, we have

$$\mu = 1 + \chi_{\mathrm{m}} (1 + H/H_{\mathrm{h}})^{-1}, \quad \chi_{\mathrm{m}} = M_{\mathrm{s}}/H_{\mathrm{h}}. \tag{13}$$

To determine the field strength H inside the layers, we use various approximate approaches. In the simplest case, it can be taken as equal to the external field strength $H = H_{\mathrm{h}}\xi$. On the basis of the formula for the field modulus following from (3) we obtain

$$H(x) = \sqrt{H_x^2 + H_z^2} + \sqrt{L^2 + R^2 + 2LR(\cos^2 x - \sin^2 x)}. \tag{14}$$

From this it is seen that the resulting field strength inside the layer, as opposed to the external field strength, changes not only across but also along it. Averaging in various ways (13) and (14) over x, we can obtain one-dimensional permeability distributions. Assuming in (13)

$$H(x) \to \langle H \rangle = \frac{1}{\pi} \int_0^{\pi} H(x)\, dx, \tag{15}$$

we obtain medium-field approximations, which are of interest only in numerical calculations, since the integral in (15) is expressed in terms of special functions. For analytical estimates, one can use a simpler averaging. According to (14), at fixed z the field value varies over the range of $H_{\min} = L - R \le H(x) \le H_{\max} = L + R$. Assuming $H = (H_{\min} + H_{\max})/2 = L$, we obtain an approximation of the internal L-field. In particular, for the one-layer model we have

$$H(x) \to L = q_c H_h \xi, \quad \mu = 1 + \chi_m (1 + q_c \xi)^{-1}. \tag{16}$$

The parameter q_c takes into account the demagnetizing influence of the layer boundaries. At $q_c = 1$ from (16) the approximation of the external L-field follows. Equations (13), (14) in the approximation of the medium and internal L-field represent a rather complicated system, which determines the self-consistent field strength and permeability distributions. Let us explain the method of solving this system in calculating the transformation parameters by the multilayer model. By the external field the values of μ are calculated in the first approximation at the interfaces of all sublayers, then by them — the mean values of μ_* in all sublayers and the coefficients r_i for all interfaces, then by formulas (5) the transformation coefficients for all boundaries are calculated, and then the base projections

$$L_i = q_i \bar{L}_i, \quad L_{i-1} = L_i \exp(-l_c/N), \quad \bar{R}_i = s_i \bar{L}_i, \quad R_i = \bar{R}_{i-1} \exp(-l_c/N).$$

are determined. By these (with the aid of (14)) the averaged field in the vicinity of all boundaries is calculated, the refined values of μ are determined, and so on. After the necessary number of iterations we obtain the self-consistent values of μ and H.

5. Interpretation of the Experimental Results on the Basis of Quasi-Linear Models. Figure 4a shows the calculated dependences of the reflection effect on the external field strength for the thickest layer of $l_c = 19.7$ mm where the changes in the field caused by the introduction of the layer are the greatest and are registered with the least relative errors. The calculation formula follows from (11), $\Delta H_d^{\text{ref}} = s H_h \xi_d \exp(2l_d)$. As would be expressed, the experimental data lie between the limiting dependences of the one-layer model. The calculation by the multilayer model with increasing number of layers leads soon enough ($N \ge 7$) to a converging result, which makes it possible to considerably improve the description of the experimental data as compared to the one-layer model.

The experimental dependences of the screening effect on the external field strength for $l_c = 8.3$ and 13 mm have a conditional maximum at $H_{d'}^{(0)} \approx 20$ kA/m (Fig. 4b). From these data it may be concluded that the value of the conditional maximum depends nonmonotonically on the layer thickness. At $l_c \approx 13$ mm the absolute maximum ($\Delta H_{\max}^{\text{scr}} \sim 3.2$ kA/m) is attained, since the dependences for both $l_c = 8.3$ mm and $l_c = 19.7$ mm lie lower than for $l_c = 13$ mm. At $l_c = 19.7$ mm the conditional maximum has not been attained because of the large thickness of the layer limiting the shift of its upper boundary into the region of fairly strong fields.

As follows from (11), the screening effect is calculated by the formula $\Delta H_{d'}^{\text{scr}} = \Delta q H_h \xi_{d'}$. As the field acting on the layer, which is characterized by $\xi_{d'}$, increases, the screening coefficient Δq decreases. The presence in the formula of two factors depending in an opposite manner on the field intensity leads to the presence of a maximum. The curves in Fig. 4b calculated by the multilayer model for wide layers (19.7 mm and 13 mm) are in good agreement with the measurement data. As the layer thickness decreases (8.3 mm and 3.3 mm), the discrepancy between the calculated and experimental data increases. This is likely to be due to the small values of the effect, which in thin layers approach the measurement error. The calculated characteristics of the absolute maximum are in good agreement with the measured ones (exceeding them by 5–10%), although they are attained at a different layer thickness (8.3 mm).

Let us investigate the extreme properties of the screening effect on the basis of the one-layer model that gives less definite, compared to the multilayer model, but better visible analytical relations for the maximum characteristics. We make an essential assumption concerning the behavior of the effective permeability in the case of change of the layer position: assume that μ_* is equal to the true permeability μ at a point fixed relative to the layer whose distance l_* from the point d' remains unchanged when the layer is displaced. Then, in the extremum condition, we can replace the variable $\xi_{d'}$ by ξ_* and write it in the form $d\Delta H_{d'}^{\text{scr}}/d\xi_* = 0$, from which it follows that

$$\Delta q_* = \xi_* \frac{dq}{dr} \frac{dr}{d\xi}, \tag{17}$$

where $\xi_* = \xi_a \exp(l_* - z_{d'})$; $\Delta q_* = \Delta q(\xi_*)$, and the values of the derivatives are taken at $\xi = \xi_*$. Taking into account that in the approximation of the internal L-field the permeability is calculated by (16), from the definition of r in (6) and (9) it follows that

$$r = \chi_m (2 + \chi_m + 2q_c\xi)^{-1} \quad \text{or} \quad r^{-1} = r_m^{-1} + 2q_c\xi/\chi_m . \tag{18}$$

Taking into account (7) and (8), from (17) and (18) we find

$$\chi_m [1 - r_*^2 \exp(-2l_c)] = 2\xi_* (2 - r_*) r_* , \quad 2\xi_* (1 - r_*) r_m r_* = (r_m - r_*) [1 - r_*^2 \exp(-2l_c)] \chi_m .$$

The solution of this system is of the form

$$r_* = 1 - \sqrt{1 - r_m} , \quad \xi_* = \frac{\chi_m}{2r_m} [1 - r_*^2 \exp(-2l_c)] .$$

It is seen that the effective reflection coefficient r_* corresponding to the conditional maximum depends only on the parameters of the magnetization curve and is not associated with the layer thickness. For the fluid used in the experiments, $\mu_m = 1 + M_s/H_h = 4.64$, $r_m = (\mu_m - 1)/(\mu_m + 1) = M_s/(M_s + 2H_h) = 0.609$, consequently, $r_* = 0.375$.

Thus, the characteristics of the conditional maximum of the screening effect at the point where the detector is positioned are determined, from the point of view of the one-dimensional model with allowance for $\xi_{d'} = \xi_* \exp(-l_*)$, by the formulas

$$\Delta H_{d'_*}^{scr} = \Delta q_* H_h \xi_{d'} = \frac{M_s r_*^2}{2r_m} [1 - \exp(-2l_c)] \exp(-l_*) , \tag{19}$$

$$H_{d'_*}^{(0)} = H_h \xi_{d'} = \frac{M_s}{2r_m} [1 - r_*^2 \exp(-2l_c)] \exp(-l_*) , \tag{20}$$

$$\Delta q_* = \frac{\Delta H_{d'_*}^{scr}}{H_{d'_*}^{(0)}} = \frac{r_*^2 [1 - \exp(-2l_c)]}{1 - r_*^2 \exp(-2l_c)} . \tag{21}$$

Expression (21) for the relative characteristic of the effect contains no uncertain parameter l_*, and the absolute characteristics (19), (20) depend on it. Assume that $l_* = nl_c + l_{d'}$. The value of $n = 1$ corresponds to the choice, as the effective permeability, of the minimum value of $\mu_* = \mu_c$ and the value of $n = 0$ — of the maximum value of $\mu_* = \mu_{c'}$. At these values of l_* (19) and (20) describe the end positions of the conditional maxima curves (Fig. 4b). The limiting curve ($n = 1$) has a maximum at a value close to the field value of $H_{d'}^{(0)} \sim 20$ kA/m at which the experimentally registered absolute maximum is observed. However, the calculated value of the reflection effect (~1.4 kA/m) is much lower than the experimental one (~3.2 kA/m). From the condition $dH_{d'_*}^{scr}/dl_c = 0$ we obtain the equation $\exp(-l_{cm}) = \sqrt{n/(n+2)}$ determining l_{cm} — the thickness of the layer at which the absolute maximum is attained. Substituting l_{cm} into (19), (20) we have

$$\Delta H_{d'm}^{scr} = \frac{M_s r_*^2}{r_m (2 + n)} \left(\frac{n}{2 + n} \right)^{n/2} \exp(-l_{d'}) , \tag{22}$$

$$H_{d'm}^{(0)} = \frac{M_s}{2r_m} \left(1 - \frac{r_*^2 n}{n + 2} \right) \left(\frac{n}{2 + n} \right)^{1/2} \exp(-l_{d'}) , \tag{23}$$

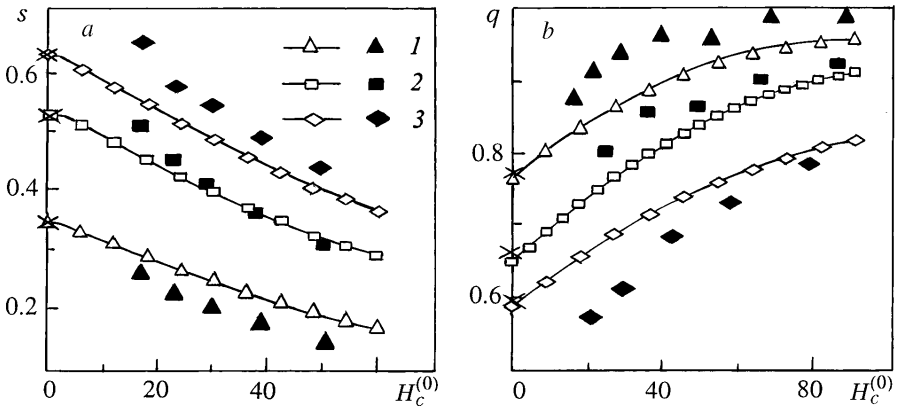

Fig. 5. Dependences of the transformation coefficients on the characteristics of the layer position in the external field for various layer thicknesses l_c: [1) 3.3; 2) 8.3; 3) 19.7 mm]. Dark symbols — results of measurements, light symbols of the same shape — results of calculation by the multilayer model.

$$\Delta q_{\rm m} = \Delta H_{\rm m}^{\rm scr} / H_{d'{\rm m}} = r_*^2 / (1 + (1 - r_*^2)\, n/2)\,. \tag{24}$$

From (22)–(24), the following limiting expressions for the absolute maximum characteristics follow:

at $n = 1$, $l_{c{\rm m}} \approx 7$ mm

$$\Delta H_{d'{\rm m}}^{\rm scr} = \frac{M_{\rm s} r_*^2}{3\sqrt{3 r_{\rm m}}} \exp(-l_{d'})\,,\quad H_{d'{\rm m}}^{(0)} = \frac{M_{\rm s}}{2\sqrt{3}} \left(1 - \frac{r_*^2}{3}\right) \exp(-l_{d'})\,,\quad \Delta q_{\rm m} = \frac{r_*^2}{1 + (1 - r_*^2)/2}\,,$$

and at $n = 0$, $l_c \to \infty$, $l_{c{\rm m}} > 40$ mm

$$\Delta H_{d'{\rm m}}^{\rm scr} = \frac{M_{\rm s} r_*^2}{2 r_{\rm m}} \exp(-l_{d'})\,,\quad H_{d'{\rm m}}^{(0)} = \frac{M_{\rm s}}{2} \exp(-l_{d'})\,,\quad \Delta q_{\rm m} = r_*^2\,.$$

The estimates of the region of parameters where the characteristics of the absolute maximum for the fluid used in the experiments should lie are as follows: $1.85 \le \Delta H_{d'{\rm m}}^{\rm scr} < 4.81$ kA/m, $18.8 < H_{d'{\rm m}}^{(0)} < 34.2$ kA/m, $0.0984 < \Delta q_{\rm m} < 0.1406$. In Fig. 4b this region is represented by a quadrangle. According to the experimental data, $\Delta q_{\rm m} \approx 3.2/20 = 0.16$, which is somewhat beyond the limits outlined by the one-layer approximation.

Figure 5 shows a comparison of the experimental values of the transformation coefficients determined by the measurement data obtained in accordance with formulas (11) with the theoretical values calculated with the use of the multilayer model. In general, the measured and calculated values are in agreement. The transmission-coefficient agreement is somewhat worse than the reflection-coefficient agreement, which is explainable: the transmission is determined by the screening effect which is weaker than the reflection effect.

The general character of the dependences given in Fig. 5 is explained by the decrease in the permeability with increasing strength. In weak fields ($\xi << 1$), μ reaches its maximum value $\mu = \mu_{\rm m} = 1 + \chi_{\rm m}$ and the layer is characterized by a maximum reflection coefficient and a minimum transmission coefficient that are exactly calculated by formulas (6) and (8). These values marked in Fig. 5 along the coordinate axis are limiting values of the dependences calculated by the multilayer model.

As the field is increased (by placing the layer closer to the source), there is a monotonic decrease in the reflectivity and, accordingly, an increase in the transmission capacity. In strong fields at $\xi >> 1$ and $\mu \to 1$, the reflection coefficient tends to zero and the transmission coefficient tends to unity.

CONCLUSIONS

The above quasi-linear models of transformation of the spatial harmonic of the magnetostatic field under interaction with a nonlinearly magnetizable medium take into account only one of the two types of fluid-induced field sources associated with the jump in the normal component of the field magnetization at the interfaces between layers with a different permeability. The second type, associated with the permeability inhomogeneity in the fluid volume in the one-layer model, is ignored, and in the multilayer models it is taken into account only partially. Nevertheless, such an approach makes it possible to form a fairly adequate idea about the transformation effect and is the basis for further development of the problem. In particular, of interest are the increase in the accuracy of measurements and the widening of their range, the account in the theory of volume field sources, and experimental and theoretical studies of the higher harmonics in reflected and transmitted fields.

The noticeable deviation of the experimental estimate of the maximum value of the screening coefficient $\Delta q_{\mathrm{m}} = 0.16$ from the theoretical limit of the quasi-linear theory (which is 0.14 for the investigated fluid) cannot, obviously, be explained on the basis of a more precise nonlinear theory either and points to the presence of some inhomogeneity of the sample. Therefore, experimental and theoretical studies of the fine laws of magnetostatic field transformation are important for the development of methods of investigation of the structure of magnetic fluids themselves.

NOTATION

H, magnetic field strength, kA/m; *M*, magnetization of the material, kA/m; μ, magnetic permeability; χ, magnetic susceptibility; *L*, *R*, base projections of the field, kA/m; ξ, dimensionless external field; *r*, harmonic reflection coefficient from a homogeneous semispace; *s*, harmonic reflection coefficient from a layered semispace; *q*, harmonic transmission coefficient through the interface; *l*, layer height, mm; λ, spatial period of the field distribution, mm; *x*, *z*, coordinates. Indices: s, saturation state; h, halved magnetization of the material; *a*, upper boundary of the magnetic layer; f, ferromagnetic; *c* and c', lower and upper boundaries of the magnetofluid dispersion layer; *d*, sensing element of the magnetic induction meter, probe; *, characteristic value; m, conditional maximum; (0), external field; max and min, maximum and minimum values; ref, reflection effect; scr, screening effect; $'$, for the upper layer.

REFERENCES

1. L. D. Landau and E. M. Lifshits, *Electrodynamics of Continua* [in Russian], Moscow (1957).
2. A. N. Vislovich, in: *Proc. 8th Int. Conf. on Magnetic Fluid*, Timisoara, Romania (1998), pp. 279–280.
3. A. N. Vislovich and A. B. Sukhotskii, *Tr. BGTU, Ser. Fiz.-Mat. Nauk* (Minsk), Issue VII, pp. 78–91 (1999).
4. A. N. Vislovich and A. B. Sukhotskii, in: *Proc. 9th Int. Pless Conf. on Magnetic Fluids* [in Russian], Vol. 1, Pless, Russia (2000), pp. 70–75.
5. A. N. Vislovich, *Magn. Gidrodin.*, No. 2, 54–60 (1990).
6. A. N. Vislovich and A. B. Sukhotskii, *Izv. Ross. Akad. Nauk, Mekh. Zhidk. Gaza*, No. 6, 3–14 (2001).